Results in Physics 14 (2019) 102442

Contents lists available at ScienceDirect

Results in Physics

journal homepage: www.elsevier.com/locate/rinp

Microarticle

Addressing the effects of background plasma and wake formation on nanosatellites with electric propulsion using a 3D Particle In Cell code

A.J.R. Lopez-Arreguin*, E. Stoll

Institute of Space Systems, TU-Braunschweig, Hermann-Blenk-Strasse 23, Braunschweig 38108, Germany

ARTICLE INFO

Keywords:
PIC
Plasma
LEO
CubeSat

ABSTRACT

3D-PIC (Particle In Cell) simulations were performed to emulate the dynamics and collection of plasma particles onto the surface of the UWE-IV, a satellite of miniaturized dimensions (CubeSat) launched in 2018. We review the electrostatic potential, currents collected and plasma disturbances of the CubeSat and characterize them by numerical simulation over Low Earth Orbits (LEO), in two general cases: as a passive satellite and with active thrusters without regard of neutralization units.

During one orbital period the passive CubeSat drives an isotropic impingement of plasma electrons, that (because their higher mobility regarding ions) govern a negative surface potential. However, by the time-evolution of the charge sheath, we relate that potential barriers may be forming around the satellite that can reduce the collection of electrons over spacecraft surfaces.

When thrusters are fired, spacecraft becomes more negatively charged than for a passive satellite, and their potential energy E_{sc} is about hundreds of times larger than the ambient ion flowing energies, E_i. In this case, ion density maps of ambient oxygen (O^+), show particles fill in the ion void (wake) zone due to bare electrostatic attraction by a (growing) negative satellite potential. The experiment was repeated in different orbit altitudes with varying plasma densities, showing that in space zones with greater concentration of plasma ions, the satellite potential is less negative, ultimately linked to this near-wake ion-focusing collection.

Thus, we conclude that if thrusters operate in LEO altitudes, where the relatively higher plasma concentrations are (equatorial orbits of 300–500 km), large negative potentials can be avoided due to the natural rule of ambient ion dynamics. This study can be important for operations of future miniaturized satellites using this type of thruster technologies.

1. Introduction

A plasma is an ionized gas macroscopically neutral [1]. As plasmas made up the entire Universe, in space and beyond the solar system we find a great variety of natural plasmas. Now, consider a body orbiting in the Earth vicinity, such that it is small enough that it has no significant atmosphere of its own: a dust grain, meteor, or even a spacecraft. Its surface is exposed to environment and continuously being bombarded by surrounding plasma and radiation that lays in space in the form of charged particles and photons. Usually, particles of relatively low energy (below few tens of keV) have a penetration depth small enough to be considered to stay in the spacecraft surface promoting charging [2]. If the energies are higher, particles can traverse the spacecraft developing deep charging of dielectric materials. This process is known as deep dielectric charging. Surface charging theory has been very well consolidated in satellites by several authors like Beard and Johnson [3], Chopra [4], Whipple [5] or Garret [6]. On the other hand, some teams like Engwall et al. [7] and Tajmar [8] (both provide a good overview on the field), observed that the use of satellite electric propulsion (EP) systems escalate the complexity of the interaction among space vehicles and ambient plasmas. EP thrusters can allow satellite buses to have more precise position control, but if not neutralized, their emissions can promote additional surface charging. Electrostatic potentials far greater than the breakdown voltage of spacecraft's materials may appear, introducing discharge arcs that risk the survival of the satellite [9]. Given the interaction of space plasma with circulant objects is critical for satellite mission control [10,11], the latest systems for EP are tested at spacecraft or instrument level [12], and simulation level (e.g. [13]). The simulation of this phenomenon has taken very important steps recently to help reducing any risk for operational failure [14,15]. In previous research, numerical simulation of the surface charging phenomena and plasma disturbances (wake or sheath formation), were

* Corresponding author.
E-mail address: amenosis.lopez@tu-braunschweig.de (A.J.R. Lopez-Arreguin).

https://doi.org/10.1016/j.rinp.2019.102442
Received 10 March 2019; Received in revised form 9 June 2019; Accepted 11 June 2019
Available online 20 June 2019

restricted mostly to medium satellites (mass of 500–1000 kg) or minisatellites (100–500 kg). The team from the Swedish Institute of Space Physics [7,16,17], presented reasonable numerical agreements with observational data of surface potential and (ion) wake formation of Cluster satellites, while facing solar wind. Furthermore, Eriksson et al. [18] reported that spacecraft's wake in sunlight can grow in size as many times the spacecraft dimensions. Hilgers et al. [10] simulated the variation of the SMART-1 spacecraft potential as a function of the orientation of the solar array, finding some surfaces acting as electron collectors drive the satellite to very high negative values. The team of Roussel [13] modeled the Microscope FEEP (Field-Effect electric Propulsion) thrusters addressing the contamination by Cesium deposit on the spacecraft surfaces, and simulated a neutralization system for the spacecraft. The contamination by interaction of ion-thruster effluents was reviewed by Roy et al. [19–21] using a PIC (Particle-in-Cell) code. Massellin reports the development of a code for modeling the SMART-1 interactions with space when using EP thrusters [22]. The team of Daotan et al. [23] typifies the potential of an spacecraft of very large dimensions depending on the plasma collection area, the emission of photocurrents, background electron temperature and shape of the satellite. Yet, the miniaturization of satellite buses and associated systems (e.g. electronics, solar arrays, thrusters, payloads), have brought the need to study charging in Low Earth Orbits (LEO) with smaller spacecraft (nanosatellites or CubeSats [24], featuring 1000 cm^3 and masses no greater than 3 kg). In this regard, it is little known the influence of LEO plasma over Cubesats with EP thrusters. Lopez et al. [25] showed that for CubeSats with EP, the simulated surface potential is dependent on the current emitted by the ion guns, the more current the more negative potential. Albarran [26] reported that in low LEO orbits, passive CubeSats (with no EP) can reach numerically an steady surface potential that is independent of the plasma density, employing the thick-sheath limit for approximation of the simulation. Thus, it is the task of this report to review the influence of the plasma environment on the electrostatic potential of an specific nanosatellite mission, that incorporates new generation EP thrusters (NanoFEEP). Based on previous tests at instument level of the propulsion system [27], the effects of background plasma, wake formation, and sheath expansion will be addressed on the UWE-IV (University Wuerzburg Experimental-IV) CubeSat.

2. Modeling of surface charging

2.1. The UWE-IV CubeSat thrusters

The UWE-IV CubeSat will employ miniaturized FEEP thrusters (called NanoFEEP), based on Gallium Liquid-Metal Ion Sources (LMIS), able to provide high accuracy orbital maneuvering within the constraints of power consumption for small satellites. The NanoFEEP is basically an ion-emitter, in which the reaction force to the electrostatic acceleration of primary Ga^+ ions provides a net thrust into the satellite platform acting in opposite direction of the net ion movement (Fig. 1). A good overview of the physics of this ion-emmitter is presented in [27]. Table 1 shows the characteristics of the thrusters of the UWE-IV Cubesat.

One of the UWE-IV constraints is to predict and control the surface floating potential of the platform, to avoid detrimental effects in spacecraft as consequence of electrostatic discharge events (ESD): material damage, operational interference [5], or disturbances to spacecraft subsystems [6]. The plasma collection issue in several mission scenarios is addressed in Section 3. By now we will review the theory of charging phenomenon.

2.2. Probe theory to describe surface charging

The historical roots of spacecraft charging analysis lie in the electrostatic probe work performed by Langmuir [28,29]. We begin with the notion that the surface charge of an orbital object is ruled by the sum of the main currents collected from the space environment:

$$I_e(\phi) - [I_i(\phi) + I_{bse}(\phi) + I_{se}(\phi) + I_{si}(\phi) + I_{ph}(\phi) + I_{th}(\phi)] = I_T \tag{1}$$

where ϕ is the body potential and I_T the total current. Following, I_e is the incident electron current, and I_i the incident ion current. I_{bse} is the backscattered electron current due to electrons, I_{se} the secondary electron current due to electrons, I_{si} is the secondary electron current due to ions, and finally I_{ph} and I_{th} are the photoelectron currents and the active current sources from the EP thrusters, respectively. A rough definition including lower magnitude current effects can be found in [5]. In the following, for a passive object ($I_{th} = 0$) only the main currents I_e and I_i are treated, resembling the typical case scenario for worst negative potentials ($I_{ph} = 0$ in eclipse and all secondary electron emissions will turn the satellite more positive). Assuming the spacecraft is a conducting sphere immersed in an isotropic Maxwell-Boltzmann plasma as found in space, the first-order currents I_{io} and I_{eo} to the satellite are given by [6]:

$$I_{\alpha o} = 2\pi\, r_{sc}^2\, q_\alpha N_{\alpha o}\left(\frac{2T_\alpha}{\pi\, m_\alpha}\right)^{(1/2)} \tag{2}$$

where r_{sc} is the satellite radius, α represent the plasma species, q_α the charge, $N_{\alpha o}$ the first-order species densities, and T_α and m_α are the temperature and mass of the plasma species (respectively). In equilibrium conditions ($I_T = 0$), the spacecraft potential ϕ_{sc} can be developed from Eqs. (1) and (2) by:

$$\phi_{sc} = \frac{-T_e}{e} ln\left(\frac{I_{eo}}{I_{io}}\right) \tag{3}$$

with e the elementary charge. For an spherical object of radius $r_s = 0.1$ m, the surface potential ϕ_{sc} can be as large as 0.4 V negative [6]. Even analytical probe theory is applicable to a number of practical problems, it has not been extended much beyond spherical or cylindrical geometries, nor does it take into account plasma disturbances [6]. In general, a body in LEO develops a space charge sheath which may be evaluated a priori to obtain the currents to the satellite. That involves computing the Poisson Equation for the potential distribution ϕ:

$$-\nabla^2\phi = \frac{e}{\epsilon_0}(N_i - N_e) \tag{4}$$

where ϵ_0 is the dielectric permitivity in space, and the particle densities follow $N_i = \int f_i\, d^3v$ and $N_e = \int f_e\, d^3v$ (e.g. N_α is found integrating the distribution function $f_\alpha$for the particle α in the velocity space v). Thus, to solve the previous formula, the collisionless-Boltzmann (Vlasov) equation shall be computed formerly for each of the species:

$$\boldsymbol{v}\cdot\nabla f_\alpha - \frac{q_\alpha}{m_\alpha}\nabla\phi(r)\cdot\nabla_v f_\alpha = 0 \tag{5}$$

where ∇ and ∇_v are the gradient operators for position and velocity space respectively, and $\boldsymbol{v}$ is the velocity vector of the plasma species [1]. Notice $\phi(r)$ takes the value of ϕ_{sc} on the satellite. The previous formulation (e.g. seeking self-consistent solutions for Eqs. (4) and (5)) was first proposed as early as 1961 in the work of Bernstein et al. [30], allowing to explain the Explorer 8 measurements over two years later [31]. Typically, an iterative procedure must be developed numerically to find the satellite potential relying on large computer codes that incorporate the sheath structure, its effects on charging currents, time characteristics or complex satellite geometries (including dielectrics most of the time). One of this codes available is SPIS version 5.0 released in 2015 [32], that uses the basic concepts of analytical probe theory, allowing end users to explicitly consider plasma simulation with satellites with high fidelity.

2.3. SPIS implementation

SPIS is a three dimensional PIC (3D-PIC) open-source code that allows the simulation of most spacecraft-plasma interactions in space

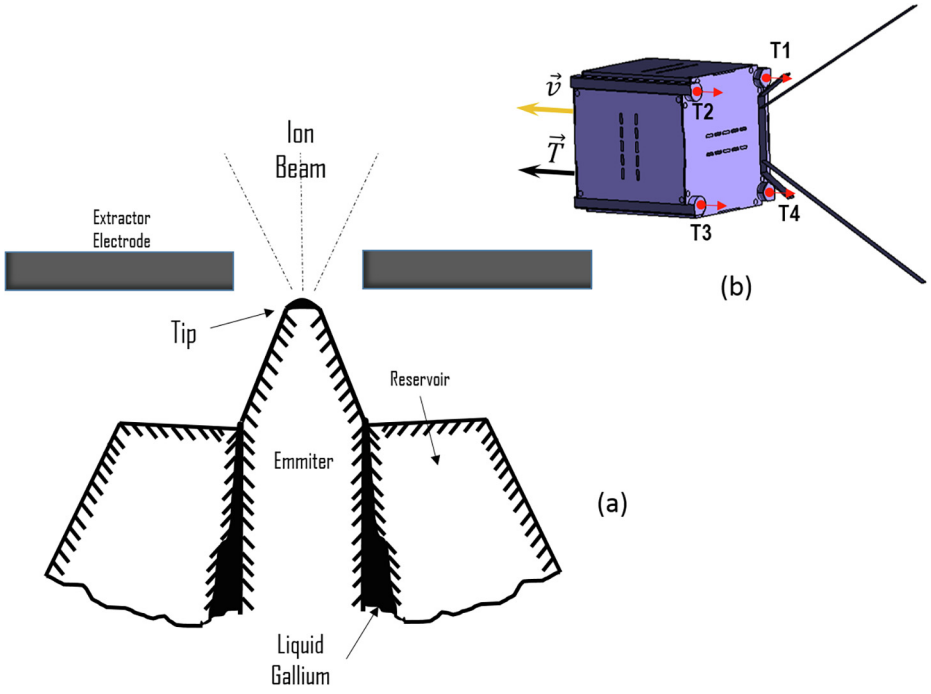

Fig. 1. NanoFEEP principles. Four thrusters (T1–T4) are arranged in the back of the satellite to provide thrust.

Table 1
Selected characteristics of the NanoFEEP thrusters.

Item	Specification
Propellant	Gallium (Ga^+)
Thrust	0.05–22 μN
Thruster operating currents (I_{th})	0–250 μA
Specific Impulse	6000 s
Maximum operating time	1800 s
Mass	6 g

[14]. Fig. 2(a) shows the digitalized model (CAD) of the UWE-IV and the computational box where all plasma is injected. There are four NanoFEEP thrusters placed in the back of the spacecraft, located around the corners. Besides, antennas for communication with ground. The interactions of the environment and the surface vehicle are computed by SPIS using an unstructured tetrahedral mesh to model the plasma volume [14]. To allow more reallistic representation of the plasma collection, the mesh spatial resolution around the thrusters and near spacecraft surfaces is increased. The plasma flux is ruled by the injection of particles into the computational box (Fig. 2(b)), and both species (electrons and ions) are modeled by Maxwellian functions. The Particle-in-Cell scheme (PIC) [32], represents a number of physical ions by macroparticles that are injected from each boundary element of the box towards randomly chosen locations inside, following a drifting Maxwellian. The initial position and velocities of such macroparticles are determined using a Monte Carlo technique [15]. On the other hand, to save computational resources, electrons are not modelled fully kinetically (full PIC) using Vlasov equation, but as a fluid instead following the typical Maxwell-Boltzmann model:

$$N_e = N_0 exp\left[\frac{e\phi}{k_B T_e}\right] \tag{6}$$

where k_B is the Bolzmann constant. N_0 is the initial undisturbed plasma density (e.g. at 0 V potential). Eq. (6) is often exact if spacecraft is not expected to become highly positive charged as typically in LEO altitudes [11].

Potential is computed by an implicit Newton-type solver for the Poisson Equation, with Dirichlet boundary conditions for the spacecraft [32]. Based on a pre-sheath model, the potential is decreased at $1/r^2$ across the length distance from the spacecraft. In the computational box, boundaries conditions follow a Robin model (mixed Dirichlet-

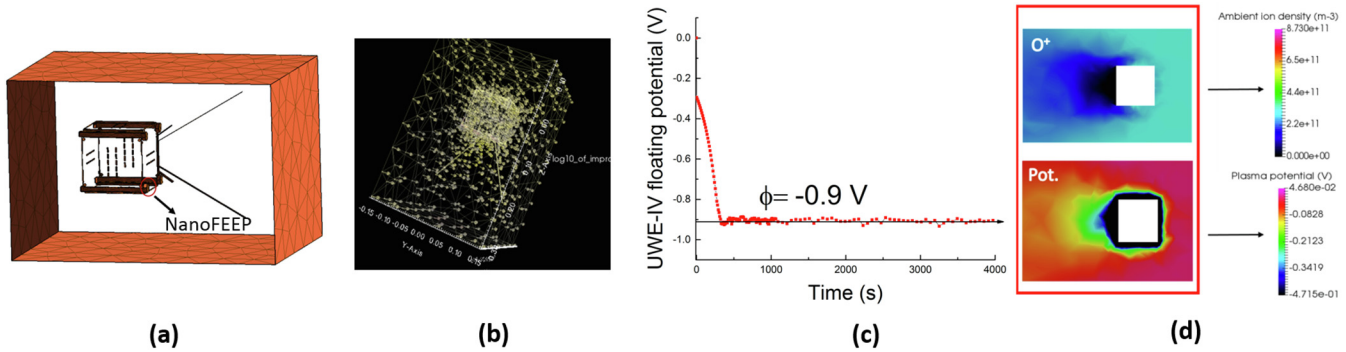

Fig. 2. (a) Implementation of the simulation box. (b) Generation of the Maxwellian plasma flow on the CubeSat. (c) Steady surface potential for a passive satellite in LEO 600 km. (d) Wake of ions formed behind the passive CubeSat displayed by the ion density maps, along the sheath expansion shown in the plasma potential map. The spacecraft traveling direction is to the right.

Neumman) [11]. Later, the currents from LEO plasma are collected by tracking the particles from injection into the computational box till they reach the surface of the UWE-IV (in case they are collected). The process is known as forward tracking, and normally ensure the ions in transit accomplish several travels through the box. To deal with dielectric surfaces, SPIS generates an spacecraft equivalent (electrical) circuit, based on continuous components representing dielectric coatings, such as resistors and capacitors [13,14]. This circuit is obtained from the material properties of the spacecraft, and to model the general satellite electrical behavior, numerically a global circuit equation is computed at self-regulated time steps.

2.4. SPIS ion dynamics

Because solving the Vlasov-Poisson system requires integrating the trajectories of millions of real particles, to determine the position and velocity vectors at each time, a less-computational demanding approach consist in tracing the equations of movement of macroparticles representing a number of physical ions. That way we must derive [17]:

$$m_\alpha \frac{d\boldsymbol{v}_n}{dt} = q_\alpha (\boldsymbol{E} + \boldsymbol{v}_n x \boldsymbol{B}) \tag{7a}$$

$$\frac{d\boldsymbol{r}_n}{dt} = \boldsymbol{v}_n \tag{7b}$$

for each macroparticle n, where α represents the macroparticle species. In general, $\boldsymbol{E}$ is considered as the dynamical electrostatic field, $\boldsymbol{B}$ is taken as user defined value and all the rest of parameters are introduced as above. The later equations are integrated using a leap frog method [33]. After the Poisson and Eq. (7) is solved, Vlasov equation is evaluated to obtain the distribution function of the species f_α, and continue the iteration process. Now, it is important to highlight the mesh is composed of 8500 tetrahedrons to model the plasma volume. Further, in SPIS each process of the simulation is solved in a spatio-temporal grid, meaning equations are evaluated for each time step within the individual surface or volume cells of the mesh.

3. Influence of the LEO plasma: results and discussion

3.1. Surface charge with inactive thrusters

An initial study of the satellite potential as a passive body was performed by SPIS. The time behaviour of the surface potential of the UWE-IV is presented in Fig. 2(c), converging to an steady state value around $\phi_{sc} = -0.9$ V, after one orbit revolution. The LEO plasma environment was introduced for a circular orbit of 600 km altitude [34], with density 10^{11} m^{-3}, temperature 0.223 eV, and satellite speed of 1780 m/s. Given the satellite velocity v_s relative to the plasma is superior than the ambient ion thermal speeds ($v_s > v_i$), a wake of ions will form behind the vehicle [7]. In addition, the higher mobility of electrons relative to the satellite (or $v_e > v_s$), will provoke the isotropic collection of negative species, while ions are collected slowly in few preferential directions [5] (e.g. $I_e > I_i$). Therefore, this will result (simultaneously) in a wake zone formation, along a negative potential structure extending further than the spacecraft dimensions. That is shown in Fig. 2(d) with the ion density and plasma potential map compiled at the final time of the simulation (approximately one orbital period). In another study, Sen et al. [35] employing SPIS, reviewed the surface charge of passive spherical debris objects orbiting in LEO and Geostationary Orbits (GEO), comparing their potential results to those provided by simple Orbital-Motion Limited (OML) theory, typically finding -1 V in LEO. However, OML theory is not applicable to LEO given the Debye length λ_D (defined as $\lambda_D = (\epsilon_0\, k_B T_e / N_0 e^2)^{1/2} \approx 0.3$ mm in LEO) is low compared to the spacecraft radius [36], commonly known as thin-sheath limit. Thus an analytical comparison which such theory seems inadequate. The spacecraft potential estimation can be oversimplified using first order current densities (given the satellite travels at high speed v_s, the ion collection in the ram region in front of the vehicle can be approximated by $I_{io} = \pi r_{sc}^2 q_i N_i v_s$ [6]), and from Eq. (3) we obtain $\phi_{sc} \approx 0.5$ V negative. Notice that past measures of electrostatic potentials in LEO agree with the estimations (-0.71 to -0.91 V between 600 and 900 km for Explorer 31 [37], -0.7 V between 400 and 650 km for OGO 4 [38], or -0.1 to -1.3 V between 275 and 600 km for AE-C [39,40]).

We can verify that the spacecraft sheath, wake formation and their time evolution can be correlated to the surface potential using the SPIS code. We will analyze the previous plasma disturbances in depth in the following section.

3.2. Influence of LEO plasma with active thrusters

The study of thruster activation in space scenarios is part of the surface charging mitigation procedures that has been initiated before by the team of the UWE-IV [25]. Because the surface potential can be regarded to a merely addition of currents, we must be very prudent to watch the firing of the ion sources that would trigger higher surface charging than the observed for a passive object [25]. A newer scenario for analysis relates the evaluation of the influence of the orbit radius over the satellite potential, when NanoFEEP are activated at nominal current ($I_{th} > 0$). That is, because the CubeSat will have to reach (self-propelled) the desired orbit from an initial release, thus interacting with the different plasma characteristics observed in space. When thrusters are activated in the simulation, SPIS generate a volumetric distribution of Ga^+ ions around the NanoFEEP, following a Maxwellian velocity distribution $f_i(v)$ drifted to the Gallium thermal velocity $v = v_{Ga}$. The beam effluent is accelerated from the LMI source by the potential drop between the emitter and electrode [41], and their velocities are related to the voltage of the beam ξ, which is the voltage of the emitter. The energy of the ion beam is thus:

$$E_{Ga} = \frac{1}{2} m_{Ga} v_{Ga}^2 = e\,\xi \tag{7c}$$

where m_{Ga} is the Gallium ion mass. The equivalent ion energies E_{Ga} for the present thruster type, have been measured experimentally in the range of 9–19 keV [27], and similar values have been adopted in the simulations. Now, we will assume the NanoFEEP are emmiting a constant current of ions of 26 μA, equivalent to generate a thrust of 2 μN approximately according the global satellite characteristics [27]. The large electron flowing speeds influence a negative surface potential because of the ratio of collected currents is $I_e/I_i > 1$ ($|I_e|$ can be as large as 213μA and I_i up to 20.4 μA [25]). Thus we could perhaps conclude that in places where the plasma density (N_0, set as equal for electrons and ions [34]) is higher, the surface potential could be more negative by product of such considerable collected electron currents I_e. We will see if this hypothesis hold. In LEO, the CubeSat will move through a dense plasma with very low temperatures (of no more than 0.3 eV as shows Fig. 3(a)). A steady surface potential were predicted and displayed in Fig. 3(b) along the respective N_0 values in the LEO range of 200–800 km. It is noticeable that at larger plasma densities (i.e. at equatorial longitudes of 300 km with a peak in plasma density of 10^{12} m^{-3}), steady potentials ($\phi_{sc} = -12$ V) are around 58 V more positive than at 700 km ($\phi_{sc} = -60$ V), where the lowest density is registered (2×10^{11} m^{-3})). Contrary to what we expected, larger plasma densities are associated with more positive surface charge. To explain this, we shall look at the dynamics of the ambient species first:

(i) Because the thruster plume is emitting currents (of $I_{th} = 26$ μA), the satellite naturally shall attract more electrons from the ambient than previously observed when $I_{th} = 0$, in order to balance the currents from Eq. (1). Thus, the spacecraft will reach an steady potential which is more negative than for a passive satellite, with a respective potential energy $E_{sc} = e\,|\phi_{sc}|$ in the range of 10–60 tens of

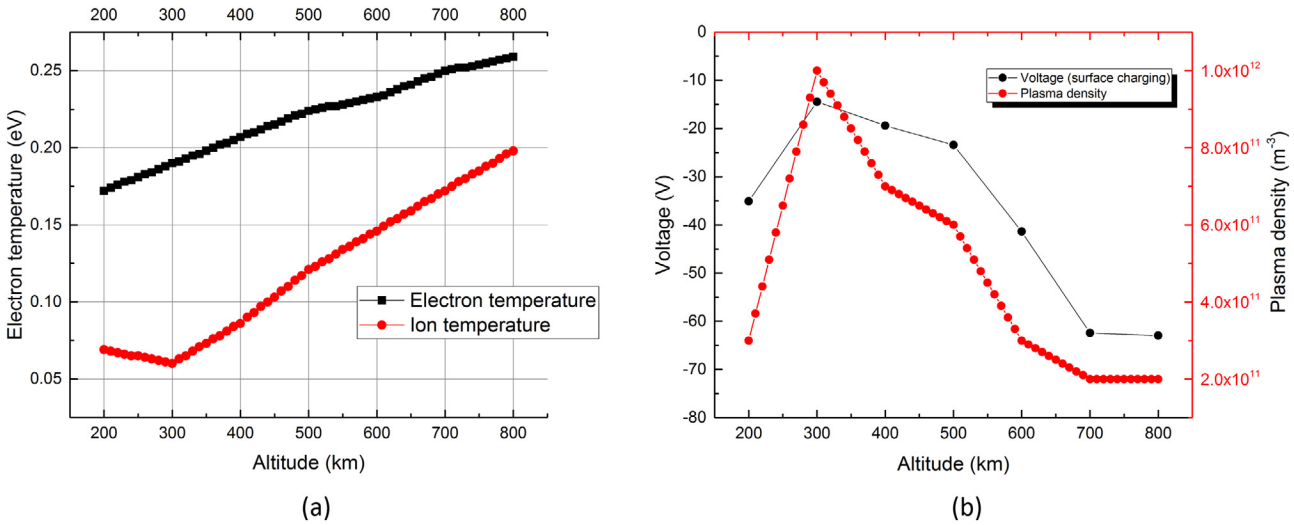

Fig. 3. (a) Plasma temperature at Low Earth Environment [34] and (b) plasma density N_0 along the associated surface charge in LEO. The values range ϕ_{sc} among $[-10, -60]$ V, with respective potential energies E_{sc} ranging [10, 60] eV.

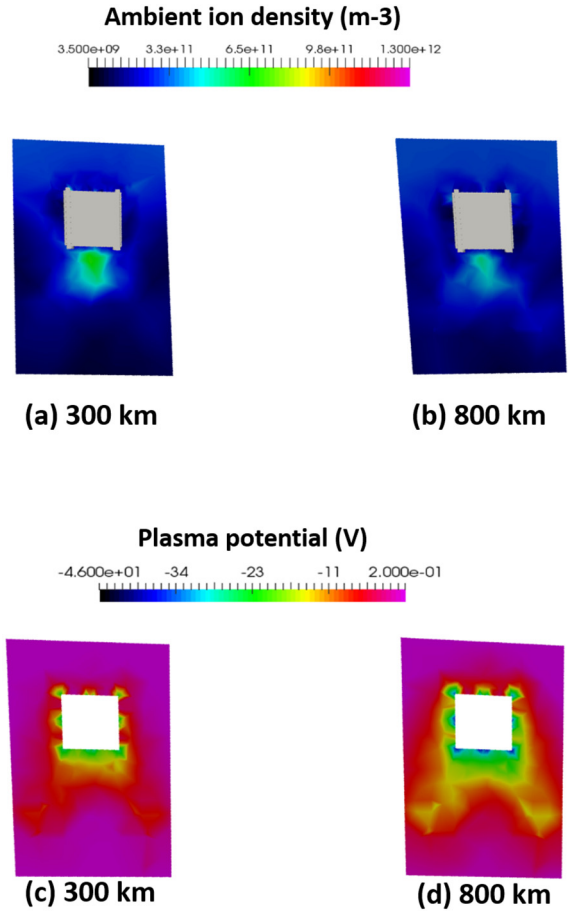

Fig. 4. Plasma potential and ambient electron densities found for the CubeSat at different altitudes. The spacecraft traveling direction is upwards.

eV (Fig. 3(b)). On the other hand, O^+ ions are randomly collected with flowing energies $E_i = k_B T_i$, of few tenths of eV as shown in Fig. 3(a). Morgan et al. [42] (and lately suggested by other simulation work [25]) reported an ion collection enhancement in the wake region whenever $E_{sc} \gg E_i$, after biasing the potential of an aluminium disc to ≈ -25 V into a focused pulsed plasma stream similar to LEO characteristics. That process seems to happen in Fig. 4(a) and (b), where the ambient ions fill the wake zone (located in opposite side of the traveling direction of the satellite). Further, this saturation of positive charges seems to be covering a larger sector area with the satellite, in the case plasma densities are higher (300 km altitude), rather than in lower density zones (800 km). Hastings et al. [43] also reviewed an unusual peak density of ions attracted in the wake, to balance the current flow of SPREE orbiter in LEO (when the potential reached -46 V). Thus it seems ions are being focused into the wake region due to the high negative surface potential the satellite acquires.

(ii) On the other hand, the negative charged species start forming around the traveling vehicle potential barriers, making the sheath to grow in size whenever electrons cannot penetrate into [5]. This process is known as sheath expansion and represented in Fig. 4(c) and (d), happening simultaneously to the ion-wake zone saturation. At this point in time electrons cannot be collected isotropically such evident due to the potential barriers [5].

In general, the time behavior of the plasma disturbances (sheath and wake structure), will provoke the satellite potential to start to be ruled by the ions found in the environment mostly, given (in time) the electron collection can be significantly decreased by the sheath expansion [5,25]. The previous can explain, why whenever we deal with higher plasma densities in LEO, the satellite could attain a more positive potential than the observed in lower plasma regions, product of the larger reservoir of ions found in the ambient. Numerically the steady potential our Cubesat could acquire saves strict relation with the plasma density, although an analytical formulation is impossible given the lack of a general probe theory to describe temporal behavior and dynamic wake phenomenon in the thin sheath limit.

4. Conclusions

The UWE-IV is a CubeSat concept that shall test miniaturized FEEP thrusters for attitude and orbit control in space. In this regard, knowledge of the surface voltage is a fundamental issue for the safety of most spacecraft operations and mission control. Charging eventually described by analytical probe theory is not applicable when considering: (1) time variations in the sheath structure, (2) effects of the satellite sheath over particle trajectories, (3) variety of surfaces, given does not explicitly consider the problem satellites consist in multiple dielectrics and other materials, and (4) differential charging. Thus complex plasma interactions were assessed through numerical simulation employing the

code SPIS. Activation of the ion thrusters were simulated generating a drifting Maxwellian function for the primary effluent particles of the NanoFEEP. A similar approach was used to emulate the ambient plasma dynamics. As result of the current balance, we observed first the potential is substantially more negative compared to a passive satellite when NanoFEEP are active. In particular, the overall negative gain effect is ameliorated when thrusters are fired in regions with increased plasma density, because the natural rule of ion dynamics collected in the near-wake. This was corroborated by distinct estimations of the spacecraft potential at different altitudes, previous reported observations, and multiple ion density and ambient potential three-dimensional maps. Even here the effect of photoelectric emission on the spacecraft is not considered, it is concluded that in any case for low altitudes (< 1000 km), such effect is small [44]. On the other hand, other effects as experienced by larger satellites, like the contribution in currents from particles coming across the magnetic force lines, will be lower since typical electron gyroradii is about the half of CubeSat cross section. Other current sources can be considered in a following study (including neutralization currents), however the spacecraft will float always to more positive potentials, in a way that the review presented here consists on the worst-case scenario.

Acknowledgements

We acknowledge to Daniel Bock and Prof. Martin Tajmar from TU-Dresden for their useful discussions that drove the formulation of this manuscript. We also thank Instituto Potosino de Investigacion Cientifica y Tecnologica (IPICYT) through Thubat Kaal 2.0 HPC for their support of computing time. We are thankful to Prof. Sergio Montenegro and Klaus Schilling for the advice provided.

Appendix A. Supplementary data

Supplementary data associated with this article can be found, in the online version, athttps://doi.org/10.1016/j.rinp.2019.102442.

References

[1] Bittencourt JA. Springer-Verlag: New York; 2004. ISBN 978-0-387-20975-3.
[2] Lai ST. Fundamentals of spacecraft charging: spacecraft interactions with space plasmas. Princeton University Press; 2011.
[3] Beard DB, Johnson FS. Ionospheric limitations on attainable satellite potential. J Geophys Res 1961;66(12):4113–22. https://doi.org/10.1029/JZ066i012p04113.
[4] Chopra K. Interactions of rapidly moving bodies in terrestrial atmosphere. Rev Modern Phys 1961;33(2):153.
[5] Whipple EC. Potentials of surfaces in space. Rep Progress Phys 1981;44(11):1197. URL:http://stacks.iop.org/0034-4885/44/i=11/a=002.
[6] Garrett HB, Whittlesey AC. John Wiley and Sons Inc.; 2012. ISBN 9781118241400. https://doi.org/10.1002/9781118241400.ch1.
[7] Engwall E, Eriksson AI, Forest J. Wake formation behind positively charged spacecraft in flowing tenuous plasmas. Phys Plasmas 2006;13(6):062904https://doi.org/10.1063/1.2199207.
[8] Tajmar M. Electric propulsion plasma simulations and influence on spacecraft charging. J Spacecraft Rockets 2002;39(6):886–93.
[9] Carruth Jr. M, Schneider T, McCollum M, Finckenor M, Suggs R, Ferguson D, et al. Iss and space environment interactions without operating plasma contactor. 39th aerospace sciences meeting and exhibit. 2001. p. 401.
[10] Hilgers A, Thiebault B, Estublier D, Gengembre E, Amo JAGD, Capacci M, et al. A simple model of the effect of solar array orientation on smart-1 floating potential. IEEE Trans Plasma Sci 2006;34(5):2159–65. https://doi.org/10.1109/TPS.2006.883405.
[11] Mateo-Velez JC, Roussel JF, Inguimbert V, Cho M, Saito K, Payan D. Spis and muscat software comparison on leo-like environment. IEEE Trans Plasma Sci 2012;40(2):177–82. https://doi.org/10.1109/TPS.2011.2173956.
[12] Torkar K, Tajmar M. Qualification of the liquid metal ion source instruments for the nasa mms mission. IEEE Trans Plasma Sci 2013;41(12):3512–9.
[13] Roussel JF, Tondu T, Mateo-Velez JC, Chesta E, D'Escrivan S, Perraud L. Modeling of feep plume effects on microscope spacecraft. IEEE Trans Plasma Sci 2008;36(5):2378–86. https://doi.org/10.1109/TPS.2008.2002541.
[14] Roussel JF, Rogier F, Dufour G, Mateo-Velez JC, Forest J, Hilgers A, et al. Spis open-source code: methods, capabilities, achievements, and prospects. IEEE Trans Plasma Sci 2008;36(5):2360–8. https://doi.org/10.1109/TPS.2008.2002327.
[15] Roussel JF, Dufour G, Mateo-Velez JC, Thiebault B, Andersson B, Rodgers D, et al. Spis multitimescale and multiphysics capabilities: development and application to geo charging and flashover modeling. IEEE Trans Plasma Sci 2012;40(2):183–91. https://doi.org/10.1109/TPS.2011.2177672.
[16] Eriksson A, Engwall E, Prakash R, Daldorff L, Torbert R, Dandouras I, et al. Making use of spacecraft–plasma interactions: determining tenuous plasma winds from wake observations and numerical simulations. Proc. 10th Spacecraft Charging Technol. Conf. 2007.
[17] Prakash R. Simulating the cluster satellites in a cold plasma flow a numerical study of spacecraft wake formation.
[18] Eriksson AI, Gwosch K, Cully CM, Sjögren A. Wake formation by ion scattering on a positively charged spacecraft.
[19] Roy RIS, Hastings DE, Taylor S. Three-dimensional plasma particle-in-cell calculations of ion thruster backflow contamination. J Comput Phys 1996;128(1):6–18.
[20] Roy RS, Hastings D, Gastonis N. Numerical study of spacecraft contamination and interactions by ion-thruster effluents. J Spacecraft Rockets 1996;33(4):535–42.
[21] Roy RS, Hastings D, Gastonis N. Ion-thruster plume modeling for backflow contamination. J Spacecraft Rockets 1996;33(4):525–34.
[22] Masselin M. Development of a hybrid pic code for the simulation of plasma spacecraft interactions; 2012.
[23] Daotan T, Shengsheng Y, Kuohai Z, Xiaogang Q, Detian L, Qing L, et al. Particle-in-cell simulation study on the floating potential of spacecraft in the low earth orbit. Plasma Sci Technol 2015;17(4):288. URL:http://stacks.iop.org/1009-0630/17/i=4/a=288.
[24] Cubesat, origin of the new space revolution.http://www.cubesat.org/ [accessed 23.05.2016].
[25] Lopez-Arreguin A, Bock D, Humbert G, Tajmar M. Spacecraft-plasma interactions of a cubesat equipped with miniaturized feep thrusters. IAC-2017. 2017. p. 1–16.
[26] Albarran I, Robert M. Cubesat wakes in the earths ionosphere; 2015.
[27] Bock D, Ebert E, Roesler F, Koessling M, Tajmar M. Development and testing of field emission thrusters at tu dresden. 5th. Russian-German conference on Electric Propulsion 2014. p. 1–16. https://doi.org/10.1117/12.134977.
[28] Langmuir I, Blodgett KB. Currents limited by space charge between concentric spheres. Phys Rev 1924;24(1):49.
[29] Mott-Smith HM, Langmuir I. The theory of collectors in gaseous discharges. Phys Rev 1926;28(4):727.
[30] Bernstein IB, Rabinowitz IN. Theory of electrostatic probes in a low-density plasma. Phys Fluids 1959;2(2):112–21.
[31] Bourdeau R, Donley J, Serbu G, Whipple E, Jr. Measurements of sheath currents and equilibrium potential on the explorer viii satellite (1960 xi); 1961.
[32] Sarrailh P, Mato-Vlez JC, Hess SLG, Roussel JF, Thibault B, Forest J, et al. Spis 5: new modeling capabilities and methods for scientific missions. IEEE Trans Plasma Sci 2015;43(9):2789–98. https://doi.org/10.1109/TPS.2015.2445384.
[33] Birdsall CK, Langdon AB. Plasma physics via computer simulation. CRC Press; 2004.
[34] Leopold database.https://www.spenvis.oma.be/help/models/leopold.html [accessed 23.05.2016].
[35] Sen A, Tiwari SK. Charging of space debris in the leo and geo regions. 40th COSPAR Scientific Assembly. 2014. vol. 40.
[36] Chiaretta M. Numerical modelling of langmuir probe measurements for the swarm spacecraft; 2011.
[37] Samir, U. Charged particle distribution in the nearest vicinity of ionospheric satellites-comparison of the main results from the ariel i, explorer 31 and geminiagena 10 spacecraft. In: Photon and Particle Interactions with Surfaces in Space. Springer; 1973, p. 193–219.
[38] Goldan PD, Yadlowsky EJ, Whipple EC. Errors in ion and electron temperature measurements due to grid plane potential nonuniformities in retarding potential analyzers. J Geophys Res 1973;78(16):2907–16.
[39] Samir U, Brace L, Brinton H. About the influence of electron temperature and relative ionic composition on ion depletion in the wake of the ae-c satellite. Geophys Res Lett 1979;6(2):101–4.
[40] Samir U, Gordon R, Brace L, Theis R. The near-wake structure of the atmosphere explorer c (ae-c) satellite: a parametric investigation. J Geophys Res: Space Phys 1979;84(A2):513–25.
[41] Bock D, Kramer E, Bangert P, Schilling K, Tajmar M. Nanofeep on uwe platform-formation flying of cubesats using miniaturized field emission electric propulsion thrusters. In: Joint Conference of 30th International Symposium on Space Technology and Science.
[42] Morgan MA, Chan C, Cooke DL, Tautz MF. The dynamics of charged particles in the near wake of a very negatively charged body-laboratory experiment and numerical simulation. IEEE Trans Plasma Sci 1989;17(2):220–7. https://doi.org/10.1109/27.24628.
[43] Hastings D. A review of plasma interactions with spacecraft in low earth orbit. J Geophys Res: Space Phys 1995;100(A8):14457–83.
[44] Brundin CL. Effects of charged particles on the motion of an earth satellite. AIAA J 1963;1(11):2529–38.